Analysis of diffraction by surface-relief crossed gratings with use of the Chandezon method: application to multilayer crossed gratings

Gérard Granet

Laboratoire des Sciences et Matériaux pour l'Electronique et d'Automatique, Unité Mixte de Recherche, Centre National de la Recherche Scientifique No. 6602, Université Blaise Pascal, Les Cézeaux Aubière Cedex, France

Received June 2, 1997; revised manuscript received November 24, 1997; accepted December 8, 1997

A new formulation of the Chandezon method for crossed gratings is presented. In the nonorthogonal translation coordinate system, an arbitrary field in a homogeneous source-free region can be expressed as the sum of a TE field and a TM field. It is shown that the whole solution can be derived from the eigensolutions of an operator independent of the polarization. In addition, use is made of the S-matrix formalism to include multilayer coated crossed gratings with parallel faces. Numerical results are given for sinusoidal crossed gratings and pyramidal gratings. © 1998 Optical Society of America [S0740-3232(98)02005-5]

OCIS codes: 0050.2770, 050.1940.

1. INTRODUCTION

The scattering of doubly periodic or crossed gratings has been the subject of many studies. Rigorous methods for two-dimensional diffraction gratings include the finite-difference method,[1] the method of variation of boundaries,[2] rigorous coupled-wave analysis,[3–7] and the curvilinear coordinate methods,[8–10] among which the Chandezon (C) method is the most popular. From a numerical point of view, this last method and rigorous coupled-wave analysis are computationally simple. Hence only basic linear algebra operations are required: seeking eigenvalues and eigenvectors and solving linear systems. The accuracy of the results is linked with the number of spatial harmonics retained in the calculation. For diffraction by crossed gratings, the size of the matrices involved in computation is squared in comparison with that of the corresponding one-dimensional problem. Therefore it is of crucial importance to derive the smallest possible eigenvalue problem. This is achieved, with rigorous coupled-wave analysis, by using a second-order differential operator.

In an earlier paper[9] I have already presented the generalization of the C method to accommodate surface-relief crossed gratings. The original feature of this method is the use of a nonorthogonal coordinate system. An operator was derived that exhibits a polarization degeneracy. It was then possible to reduce the initial eigenvalue problem to two eigenvalue problems, the size of the associated matrices being half the size of the initial one. The aim of this paper is to present a new formulation of the C method as applied to crossed gratings. Following McPhedran *et al.*,[11] the field is decomposed into transverse electric (TE) and transverse magnetic (TM) vector fields. These are defined in the same way as is habitual in the theory of waveguides, with the direction orthogonal to the interface plane being the preferred direction.

In the previous formulation, the complete eigensolution was obtained by appealing to two different eigenequations in turn before combining the two to reconstruct the original field vector. In the present formulation, the TE and TM fields are derived from the solution of a single scalar eigenequation. It is obvious that the matrix associated with this new operator is also half the size of the initial one. From a numerical point of view, I believe that this is a great improvement, since solving the eigenproblem is the most time-consuming part of the computer code used.

Numerical examples are provided to demonstrate the effectiveness of the method. In addition, the S-matrix formalism is used to include multilayer coated crossed gratings with parallel faces, which are assimilated to planar stratified media, thanks to the new coordinate system.

2. DESCRIPTION OF THE PROBLEM AND NOTATION

The general system considered in this calculation is shown in Fig. 1. It consists of a multilayer stack with $Q - 1$ layers, labeled by $j = 1, 2, ..., Q - 1$, of refractive index ν_j and thickness e_j. The entry and exit media have refractive indices ν_0 and ν_Q, respectively. To accommodate lossy media, the refractive indices ν_j, $j = 1, 2, ..., Q$, are taken to be complex quantities. These regions are separated by Q interfaces labeled by $j = 1, 2, ..., Q$; that is, the jth layer has the jth interface as the upper boundary and the $(j + 1)$th interface as the lower boundary. The normal to the stack, in the direction of decreasing j, is the y axis. All the interfaces have an identical periodic modulation, with the period d_x in the x direction and the period d_z in the z direction. The uppermost interface is located at the origin of the y axis, so that the equation of the top surface of the jth layer is given by

0740-3232/98/051121-11$15.00

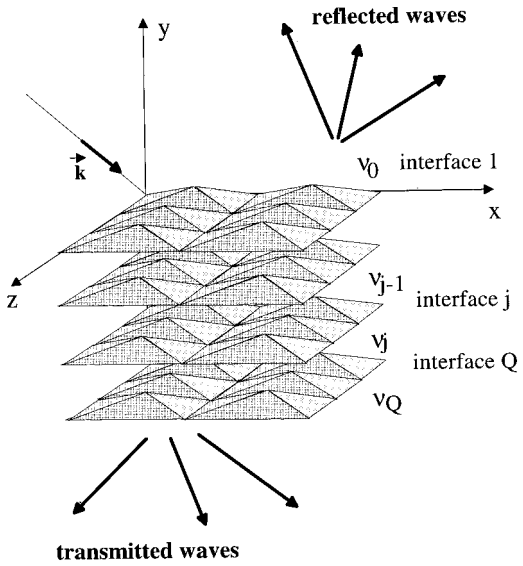

Fig. 1. Multilayer coated crossed grating.

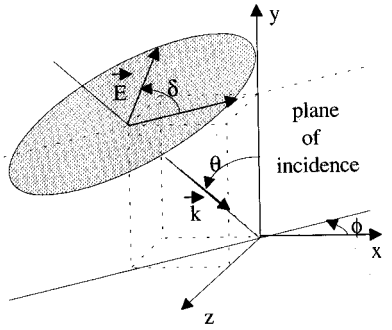

Fig. 2. Definition of the incident plane wave.

$$y_j = -\sum_{i<j} e_i + a(x, z), \tag{1}$$

where the function $a(x, z)$ represents the shape modulation. It can be expanded into a Fourier series:

$$a(x, z) = \sum_{p,q} a_{pq} \exp\left[-i2\pi\left(\frac{px}{d_x} + \frac{qz}{d_z}\right)\right], \tag{2}$$

where

$$a_{pq} = \frac{1}{d_x d_z} \int_0^{d_x}\int_0^{d_z} a(u, v) \exp\left[i2\pi\left(\frac{pu}{d_x} + \frac{qv}{d_z}\right)\right] du\, dv. \tag{3}$$

A. Incident Plane Wave

This structure is illuminated from the uppermost medium by a homogeneous monochromatic plane wave that is linearly polarized and has a vacuum wavelength λ and an angular frequency ω (Fig. 2). The $\exp(i\omega t)$ time dependence is assumed and will be suppressed throughout this paper. In the Cartesian coordinate system, the components of the wave vector $\mathbf{k}$ and those of the unit-amplitude electric-field vector $\hat{\mathbf{u}}$ are, respectively,

$$k_x = k \sin\theta \cos\phi, \qquad k_y = -k \cos\theta,$$
$$k_z = -k \sin\theta \sin\phi, \tag{4}$$

with $k = 2\pi/\lambda = \omega\sqrt{\mu_0\epsilon_0}$, where ϵ_0 and μ_0 are the permittivity and the permeability of vacuum, respectively; and

$$\hat{\mathbf{u}} = (\cos\delta \cos\theta \cos\phi - \sin\delta \sin\phi)\hat{\mathbf{x}} + (\cos\delta \sin\theta)\hat{\mathbf{y}} + (\cos\delta \cos\theta \sin\phi + \sin\delta \cos\phi)\hat{\mathbf{z}}, \tag{5}$$

where δ represents the angle between the electric-field vector and the plane of incidence.

B. TE and TM Vector Fields: Rayleigh Expansion

In what follows, we refer to the medium with the subscript j. In rectangular coordinates any wave function ψ of the form

$$\psi_j(x, y, z) = \sum_\alpha \sum_\gamma A_{\alpha\gamma} \exp[-ik(\alpha x + \beta_j y + \gamma z)] \tag{6}$$

with

$$\alpha^2 + \beta_j^2 + \gamma^2 = \nu_j^2 \tag{7}$$

is a solution to the Helmholtz equation.[12]

In our problem α and γ can be expressed as

$$\alpha = \alpha_m = \alpha_0 + m\frac{\lambda}{d_x}, \qquad \gamma = \gamma_n = \gamma_0 + n\frac{\lambda}{d_z}, \tag{8}$$

with

$$\alpha_0 = \sin\theta \cos\phi, \qquad \gamma_0 = -\sin\theta \sin\phi. \tag{9}$$

From Eq. (7), we can then deduce that

$$\beta_{j\,mn}^2 = \nu_j^2 - \alpha_m^2 - \gamma_n^2. \tag{10}$$

In bigrating problems it is advantageous to represent the electromagnetic-field components as a linear combination of two types of solutions corresponding to $E_{yj} = 0$ and $H_{yj} = 0$. We refer to these solutions, or polarizations, as TE or TM to the Oy axis. Transverse means the absence of an Oy component of the relevant field quantity. Furthermore, E_{yj} and H_{yj} satisfy separately the scalar Helmholtz equation. We write them as

$$E_{yj} = \sum_{m,n} A_{j\,mn}^{+\mathrm{TM}} \exp[-ik(\alpha_m x + \beta_{j\,mn}^{+} y + \gamma_n z)] + \sum_{m,n} A_{j\,mn}^{-\mathrm{TM}} \exp[-ik(\alpha_m x + \beta_{j\,mn}^{-} y + \gamma_n z)], \tag{11}$$

$$H_{yj} = \sum_{m,n} A_{j\,mn}^{+\mathrm{TE}} \exp[-ik(\alpha_m x + \beta_{j\,mn}^{+} y + \gamma_n z)] + \sum_{m,n} A_{j\,mn}^{-\mathrm{TE}} \exp[-ik(\alpha_m x + \beta_{j\,mn}^{-} y + \gamma_n z)], \tag{12}$$

$$\beta_{j\,mn}^{+} = \begin{cases} (\nu_j^2 - \alpha_m^2 - \gamma_n^2)^{1/2} & \text{if } \nu_j^2 - \alpha_m^2 - \gamma_n^2 \geqslant 0 \\ -i(\alpha_m^2 + \gamma_n^2 - \nu_j^2)^{1/2} & \text{if } \nu_j^2 - \alpha_m^2 - \gamma_n^2 < 0 \end{cases}, \tag{13}$$

$$\beta_{j\,mn}^{-} = -\beta_{j\,mn}^{+}. \tag{14}$$

These expansions are known as Rayleigh expansions.

Then, separating Maxwell's equations for E_{yj} and H_{yj} allows us to express the other field components as a linear combination of TE and TM vector fields:

$$\begin{aligned} \boldsymbol{\psi}_j^R = & \sum_{m,n} (A_{j\,mn}^{+\mathrm{TE}} \boldsymbol{\psi}_{j\,mn}^{+R\ \mathrm{TE}} + A_{j\,mn}^{+\mathrm{TM}} \boldsymbol{\psi}_{j\,mn}^{+R\ \mathrm{TM}}) \\ & \times \exp[-ik(\alpha_m x + \beta_{j\,mn}^{+} y + \gamma_n z)] \\ & + \sum_{m,n} (A_{j\,mn}^{-\mathrm{TE}} \boldsymbol{\psi}_{j\,mn}^{-R\ \mathrm{TE}} + A_{j\,mn}^{-\mathrm{TM}} \boldsymbol{\psi}_{j\,mn}^{-R\ \mathrm{TM}}) \\ & \times \exp[-ik(\alpha_m x + \beta_{j\,mn}^{-} y + \gamma_n z)], \end{aligned} \tag{15}$$

where

$$\boldsymbol{\psi}_j^R = \begin{pmatrix} E_{zj} \\ ZH_{xj} \\ ZH_{zj} \\ E_{xj} \end{pmatrix}, \tag{16}$$

$$\boldsymbol{\psi}_{j\,mn}^{+R\ \mathrm{TE}} = \frac{1}{\beta_{j\,mn}^2 - \nu_j^2} \begin{pmatrix} \alpha_m \\ \beta_{j\,mn}^{+} \alpha_m \\ \beta_{j\,mn}^{+} \gamma_n \\ -\gamma_n \end{pmatrix}, \tag{17}$$

$$\boldsymbol{\psi}_{j\,mn}^{+R\ \mathrm{TM}} = \frac{1}{\beta_{j\,mn}^2 - \nu_j^2} \begin{pmatrix} \beta_{j\,mn}^{+} \gamma_n \\ -\nu_j^2 \gamma_n \\ \nu_j^2 \alpha_m \\ \beta_{j\,mn}^{+} \alpha_m \end{pmatrix}, \tag{18}$$

$$Z = \sqrt{\mu_0 / \epsilon_0}.$$

Similar expressions hold for $\boldsymbol{\psi}_{j\,mn}^{-R\ \mathrm{TE}}$ and $\boldsymbol{\psi}_{j\,mn}^{-R\ \mathrm{TM}}$.

In the above relations, the superscripts + and − correspond to waves that propagate or decay in the positive or negative Oy direction, respectively. The superscript R refers to Rayleigh expansion. It can be verified that, by setting $\alpha_0 = \sin\theta\cos\phi$, $\gamma_0 = -\sin\theta\sin\phi$, $\beta_{00}^{-} = -\cos\theta$, $A_{0\,00}^{-\mathrm{TE}} = \cos\delta$, and $A_{0\,00}^{-\mathrm{TM}} = \sin\delta$, we obtain the components of the incident electric field as given by Eq. (5). Our aim is to determine the coefficients $A_{0\,mn}^{+\mathrm{TE}} A_{0\,mn}^{+\mathrm{TM}}$, $A_{Q\,mn}^{-\mathrm{TE}}$, and $A_{Q\,mn}^{-\mathrm{TM}}$, from which we shall calculate the reflected and transmitted efficiencies.

3. THEORY

A. Eigenvalue Equation

To write in a simple manner the continuity conditions of the electromagnetic field on the interfaces, we use the so-called translation coordinate system defined as follows:

$$x^1 = x, \qquad x^2 = u = y - a(x, z), \qquad x^3 = z. \tag{19}$$

The contravariant components of the corresponding metric tensor are given by

$$g^{ij} = \begin{bmatrix} 1 & -\dfrac{\partial a}{\partial x} & 0 \\ -\dfrac{\partial a}{\partial x} & 1 + \left(\dfrac{\partial a}{\partial x}\right)^2 + \left(\dfrac{\partial a}{\partial z}\right)^2 & -\dfrac{\partial a}{\partial z} \\ 0 & -\dfrac{\partial a}{\partial z} & 1 \end{bmatrix}. \tag{20}$$

According to Post,[13] Maxwell's equations take the form

$$\xi^{ijk} \partial_j E_k = -ik\sqrt{g} g^{ij} Z H_j, \tag{21}$$

$$\xi^{ijk} \partial_j Z H_k = ik\nu^2 \sqrt{g} g^{ij} E_j, \tag{22}$$

where $i, j, k \in \{1, 2, 3\}$, ν is the refractive index of the medium, ∂_j ($j \in \{1, 2, 3\}$) stands for $\partial/\partial x^j$, ξ^{ijk} is the Levi–Civita indicator:

$$\xi^{ijk} = \begin{cases} +1 & \text{if } (i, j, k) \text{ is an even permutation of } (1, 2, 3) \\ -1 & \text{if } (i, j, k) \text{ is an odd permutation of } (1, 2, 3) \\ 0 & \text{otherwise} \end{cases}; \tag{23}$$

E_j and H_k denote the complex amplitudes of the covariant components of the electric and magnetic fields, and $g = \det[(g^{ij})^{-1}]$.

Since the metric tensor components are independent of the x^2 coordinate, a system of four equations can be easily deduced from system (21) and (22); this system is expressed as

$$\partial_2 \begin{pmatrix} E_3 \\ ZH_1 \\ ZH_3 \\ E_1 \end{pmatrix} = L_{1,3} \begin{pmatrix} E_3 \\ ZH_1 \\ ZH_3 \\ E_1 \end{pmatrix}, \tag{24}$$

where $L_{1,3}$ is a linear differential operator depending only on the coordinates x^1 and x^3. It is then possible to separate the variables to find elementary solutions of the form

$$S(x^1, x^2, x^3) = S(x^1, x^3)\exp(-ikrx^2), \tag{25}$$

where S represents any of the six components of the field. Indeed, in Ref. 9, I have solved the eigenvalue equation (24). However, another solution can be derived by following two steps. First, from Maxwell's equations and thanks to the invariability of the problem along the y direction, the components with subscripts 1 and 3 can be expressed in terms of the components E_2 and H_2:

$$\begin{aligned} (\partial_2^2 + \omega^2\mu\epsilon) E_3 = & -(i\omega\mu g^{12}\partial_2 + i\omega\mu\partial_1) H_2 \\ & + (\partial_2\partial_3 - \omega^2\mu\epsilon g^{32}) E_2, \end{aligned} \tag{26}$$

$$\begin{aligned} (\partial_2^2 + \omega^2\mu\epsilon) H_1 = & (\partial_2\partial_1 - \omega^2\mu\epsilon g^{12}) H_2 \\ & - (i\omega\epsilon\partial_3 + i\omega\epsilon g^{32}\partial_2) E_2, \end{aligned} \tag{27}$$

$$\begin{aligned} (\partial_2^2 + \omega^2\mu\epsilon) H_3 = & (\partial_2\partial_3 - \omega^2\mu\epsilon g^{32}) H_2 \\ & + (\partial_2 i\omega\epsilon g^{12} + i\omega\epsilon\partial_1) E_2, \end{aligned} \tag{28}$$

$$(\partial_2^2 + \omega^2\mu\epsilon)E_1 = (i\omega\mu\partial_3 + i\omega\mu g^{32}\partial_2)H_2 + (\partial_2\partial_1 - \omega^2\mu\epsilon g^{12})E_2. \quad (29)$$

Second, after some tedious calculation, and provided that the medium is homogeneous, it can be shown that the longitudinal components E_2 and H_2 obey the same wave equation:

$$g^{22}\partial_2^2\phi + \partial_2[(g^{21}\partial_1 + \partial_1 g^{21})\phi] + \partial_2[(g^{23}\partial_3 + \partial_3 g^{23})\phi] + \partial_1^2\phi + \partial_3^2\phi + \omega^2\mu\epsilon\phi = 0. \quad (30)$$

Thus, independent of the coordinate system, an arbitrary field in a homogeneous source-free region can be expressed as the sum of a TE field and a TM field:

$$\boldsymbol{\psi} = s^{\mathrm{TE}}\boldsymbol{\psi}^{\mathrm{TE}} + s^{\mathrm{TM}}\boldsymbol{\psi}^{\mathrm{TM}}, \quad (31)$$

where $\boldsymbol{\psi}$ is a vector whose components are the functions E_3, H_1, H_3, and E_1.

Some additional calculus has to be done to deal with the particular case where $\partial_2^2 + \omega^2\mu\epsilon = 0$. This case is such that both E_2 and H_2 are equal to zero (that is, TEM polarization!). Hence the determination of the electromagnetic field amounts to solving Eq. (30) and deducing the TE and TM vector fields according to

$$(\partial_2^2 + \omega^2\mu\epsilon)\boldsymbol{\psi}^{\mathrm{TE}} = \begin{pmatrix} -(i\omega\mu g^{12}\partial_2 + i\omega\mu\partial_1)\phi \\ (\partial_2\partial_1 - \omega^2\mu\epsilon g^{12})\phi \\ (\partial_2\partial_3 - \omega^2\mu\epsilon g^{32})\phi \\ (i\omega\mu g^{32}\partial_2 + i\omega\mu\partial_3)\phi \end{pmatrix} \quad \text{if } \partial_2^2+\omega^2\mu\epsilon\neq 0,$$

$$\boldsymbol{\psi}^{\mathrm{TE}} = \begin{pmatrix} \phi \\ \pm i\omega\epsilon\phi \\ 0 \\ 0 \end{pmatrix} \quad \text{if } \partial_2^2 + \omega^2\mu\epsilon = 0; \quad (32)$$

$$(\partial_2^2 + \omega^2\mu\epsilon)\boldsymbol{\psi}^{\mathrm{TM}} = \begin{pmatrix} (\partial_2\partial_3 - \omega^2\mu\epsilon g^{32})\phi \\ -(i\omega\epsilon g^{32}\partial_2 + i\omega\epsilon\partial_3)\phi \\ (i\omega\epsilon g^{12}\partial_2 + i\omega\epsilon\partial_1)\phi \\ (\partial_2\partial_1 - \omega^2\mu\epsilon g^{12})\phi \end{pmatrix} \quad \text{if } \partial_2^2 + \omega^2\mu\epsilon \neq 0,$$

$$\boldsymbol{\psi}^{\mathrm{TM}} = \begin{pmatrix} 0 \\ 0 \\ \phi \\ \pm i\omega\mu\phi \end{pmatrix} \quad \text{if } \partial_2^2 + \omega^2\mu\epsilon = 0. \quad (33)$$

When the medium is homogeneous and the metric tensors are independent of the coordinates x^2 and x^3, two TE and TM fields are available: one to x^2 and the other to x^3. This situation is that of monoperiodic gratings, whether used in a classical or a conical mount.

B. Numerical Solution

To be solved with an eigenvalue method, Eq. (30) has to be transformed. With the introduction of $\phi' = (i/k) \times (\partial\phi/\partial u)$, it becomes a generalized eigenvalue equation of the form

$$L_{A\ 1,3}\frac{\partial}{\partial u}\begin{pmatrix}\phi\\ \phi'\end{pmatrix} = L_{B\ 1,3}\begin{pmatrix}\phi\\ \phi'\end{pmatrix}, \quad (34)$$

where $L_{A\ 1,3}$ and $L_{B\ 1,3}$ are linear differential operators depending only on coordinates x^1 and x^3:

$$L_{A\ 1,3} = \begin{bmatrix} -g^{12}\frac{\partial}{\partial x} - \frac{\partial}{\partial x}g^{12} - g^{23}\frac{\partial}{\partial z} - \frac{\partial}{\partial z}g^{23} & -ikg^{22} \\ \frac{i}{k} & 0 \end{bmatrix}, \quad (35)$$

$$L_{B\ 1,3} = \begin{bmatrix} -k^2\nu^2 - \frac{\partial^2}{\partial x^2} - \frac{\partial^2}{\partial z^2} & 0 \\ 0 & 1 \end{bmatrix}. \quad (36)$$

It is then possible to separate the variables to find elementary solutions of the form

$$\phi(x, u, z) = \phi(x, z)\exp(-ikru). \quad (37)$$

Since the function $a(x, z)$ is periodic, ϕ is a pseudoperiodic function and can therefore be decomposed into Floquet harmonics:

$$\phi(x, z) = \sum_{m,n}\phi_{mn}\exp[-ik(\alpha_m x + \gamma_n z)]. \quad (38)$$

We assume that a finite sum of these harmonics is enough to represent the function; hence

$$\phi(x, z) = \sum_{m=-M}^{m=+M}\sum_{n=-N}^{n=+N}\phi_{mn}\exp[-ik(\alpha_m x + \gamma_n z)]. \quad (39)$$

Substituting this expression into Eq. (34) and expanding the components of the metric tensor into a Fourier series as

$$g^{12} = \sum_{m,n} g_{mn}^{12}\exp\left[-i2\pi\left(\frac{mx}{d_x} + \frac{nz}{d_z}\right)\right], \quad (40)$$

$$g^{23} = \sum_{m,n} g_{mn}^{23}\exp\left[-i2\pi\left(\frac{mx}{d_x} + \frac{nz}{d_z}\right)\right], \quad (41)$$

$$g^{22} = \sum_{m,n} g_{mn}^{22}\exp\left[-i2\pi\left(\frac{mx}{d_x} + \frac{nz}{d_z}\right)\right], \quad (42)$$

with

$$g_{mn}^{12} = -i\frac{2\pi m}{d_x}a_{mn}, \quad (43)$$

$$g_{mn}^{23} = -i\frac{2\pi n}{d_z}a_{mn}, \quad (44)$$

$$g_{mn}^{22} = \delta_{mn} + \sum_{u,v} g_{m-u,n-v}^{12}g_{uv}^{12} + \sum_{u,v} g_{m-u,n-v}^{23}g_{uv}^{23}, \quad (45)$$

we obtain two sets of coupled first-order differential equations:

$$\sum_{p,q}(-g_{m-p,n-q}^{12}\alpha_p - g_{m-p,n-q}^{12}\alpha_m - g_{m-p,n-q}^{23} \times \gamma_q - g_{m-p,n-q}^{23}\gamma_n)r_j\phi_{mn} + \sum_{p,q} g_{m-p,n-q}^{22}r_j\phi'_{mn} = (\nu_j^2 - \alpha_m^2 - \gamma_n^2)\phi_{mn},$$

$$r_j \phi_{mn} = \phi'_{mn}. \tag{46}$$

These equations can be written in matrix form:

$$\mathbf{A}\mathbf{r}\begin{pmatrix} \phi \\ \phi' \end{pmatrix} = \mathbf{B}\begin{pmatrix} \phi \\ \phi' \end{pmatrix}, \tag{47}$$

where $\mathbf{A}$ and $\mathbf{B}$ are square matrices of dimension $2L$, with $L = (2M + 1)(2N + 1)$, specified by the left-hand side and the right-hand side of Eqs. (46), respectively.

Finally, in the jth medium, the function ϕ_j can be expressed as

$$\phi_j(x, u, z) = \sum_{m=-M}^{m=+M} \sum_{n=-N}^{n=+N} \sum_{l=1}^{l=2L} \phi_{j,\,mn\,l} \exp(-ikr_{jl}u) \times \exp(-ik\alpha_m x)\exp(-ik\gamma_n z), \tag{48}$$

where $\phi_{j\,mn\,l}$ is the upper part of the eigenvector of matrix $\mathbf{B}^{-1}\mathbf{A}$ associated with the eigenvalue $1/r_{jl}$.

It is observed numerically that there are two sets of modes, the number of which are equal: those propagating or decaying in the positive y direction and those traveling in the opposite direction. We denote these modes by the superscripts + and −, respectively.

The numerically computed eigenvalues and eigenvectors depend on the truncation orders M and N. In the following relation, we use two extra superscripts M and N to indicate this dependence. Numerical experiments show that, for two constants p and q,

$$\lim_{M,N\to\infty} r_{j\,pq}^{MN} = \beta_{j\,pq}. \tag{49}$$

In the above equation, we have specified the computed eigenvalues with two integers rather than one in order to compare them with the Rayleigh eigenvalues $\beta_{j\,pq}$. The interesting feature of Eq. (49) is that the limit is independent of the coordinate system. This is not surprising because in a homogeneous space the eigensolutions of Maxwell's equations are just plane waves. Indeed, provided that we substitute y for u-$a(x, z)$, it can be shown that the wave function ψ_j of Eq. (6) is a solution of the wave equation (30). However, the invariance of the eigensolutions is severely destroyed by the matrix truncation that is unavoidable in the numerical implementation. For the C method to be successful, M and N have to be chosen large enough so that the computed real eigenvalues coincide with a great accuracy with the real Rayleigh eigenvalues. Hence the associated eigenvectors coincide with plane waves expressed in the translation coordinate system. As did Chandezon *et al.*,[14] we replace, in the decomposition of the function ϕ on the $\mathbf{B}^{-1}\mathbf{A}$-matrix eigenvectors, the computed eigenvectors associated with real eigenvalues by the corresponding truncated Rayleigh eigenvectors. That is,

$$\sum_{m=-M}^{m=+M} \sum_{n=-N}^{n=+N} \sum_{p,q\in U_j} \phi_{j\,mn\,pq} \exp(-ikr_{j\,pq}u) \times \exp(-ik\alpha_m x)\exp(-ik\gamma_n z), \tag{50}$$

where

$$U_j = \{(p, q) \in [-M, M] \times [-N, N], \; \nu_j^2 - \alpha_p^2 - \gamma_q^2 > 0\} \tag{51}$$

is replaced by the truncated Fourier-series expansion of

$$\sum_{p,q} \exp\{-ik\beta_{j\,pq}[u + a(x, z)]\} \times \exp(-ik\alpha_p x)\exp(-ik\gamma_q z). \tag{52}$$

Hence the function ϕ_j takes the following form:

$$\begin{aligned}\phi_j(x, u, z) &= \sum_{m=-M}^{m=+M} \sum_{n=-N}^{n=+N} \sum_{p,q\in U_j} \phi_{j\,mn\,pq}^{+R} \exp(-ik\beta_{j\,pq}^{+}u) \times \exp(-ik\alpha_m x)\exp(-ik\gamma_n z) \\ &+ \sum_{m=-M}^{m=+M} \sum_{n=-N}^{n=+N} \sum_{p,q\in V_j^+} \phi_{j\,mn\,pq}^{+} \exp(-ikr_{j\,pq}^{+}u) \times \exp(-ik\alpha_m x)\exp(-ik\gamma_n z) \\ &+ \sum_{m=-M}^{m=+M} \sum_{n=-N}^{n=+N} \sum_{p,q\in U_j} \phi_{j\,mn\,pq}^{-R} \exp(-ik\beta_{j\,pq}^{-}u) \times \exp(-ik\alpha_m x)\exp(-ik\gamma_n z) \\ &+ \sum_{m=-M}^{m=+M} \sum_{n=-N}^{n=+N} \sum_{p,q\in V_j^-} \phi_{j\,mn\,pq}^{-} \exp(-ikr_{j\,pq}^{-}u) \times \exp(-ik\alpha_m x)\exp(-ik\gamma_n z),\end{aligned} \tag{53}$$

where

$$\phi_{j\,mn\,pq}^{\pm R} = \frac{1}{d_x d_z} \int_0^{d_x}\int_0^{d_z} \exp[-ik(\beta_{j\,pq}^{\pm})a(u, v)] \times \exp(-ik\alpha_{p+m}u)\exp(-ik\gamma_{q+n}v)\,\mathrm{d}u\,\mathrm{d}v, \tag{54}$$

$$V_j^+ = \{(p, q) \in ([-M, M] \times [-N, N] - U_j), \; \mathrm{Im}(r_{j\,pq}) < 0\}, \tag{55}$$

$$V_j^- = \{(p, q) \in ([-M, M] \times [-N, N] - U_j), \; \mathrm{Im}(r_{j\,pq}) > 0\}. \tag{56}$$

$\mathrm{Im}(r_{j\,pq})$ designates the imaginary part of $r_{j\,pq}$, $r_{j\,pq}^{+} \in \{r_{j\,pq}, (p, q) \in V_j^+\}$, and $r_{j\,pq}^{-} \in \{r_{j\,pq}, (p, q) \in V_j^-\}$. Once the eigenvalue problem is solved, the field components of interest can be easily deduced from Eqs. (32) and (33). The final form of the solution is therefore

$$\psi_j^l = \sum_{m,n\ p,q} A_{j\,pq}^{+l\ \mathrm{TE}} \psi_{j\,mn\,pq}^{+\mathrm{TE}} \exp[-ikr_{j\,pq}^{+}(u - u_l)] \times \exp(-ik\alpha_m x)\exp(-ik\gamma_n z) + \sum_{m,n\ p,q} A_{j\,pq}^{+l\ \mathrm{TM}} \psi_{j\,mn\,pq}^{+\mathrm{TM}} \exp[-ikr_{j\,pq}^{+}(u - u_l)] \times \exp(-ik\alpha_m x)\exp(-ik\gamma_n z) + \sum_{m,n\ p,q} A_{j\,pq}^{-l\ \mathrm{TE}} \psi_{j\,mn\,pq}^{-\mathrm{TE}} \exp[-ikr_{j\,pq}^{-}(u - u_l)] \times \exp(-ik\alpha_m x)\exp(-ik\gamma_n z) + \sum_{m,n\ p,q} A_{j\,pq}^{-l\ \mathrm{TM}} \psi_{j\,mn\,pq}^{-\mathrm{TM}} \exp[-ikr_{j\,pq}^{-}(u - u_l)] \times \exp(-ik\alpha_m x)\exp(-ik\gamma_n z), \quad (57)$$

where the superscript l, with $l = j$ or $l = j - 1$, refers to the lth interface.

It should be noted that we get two expressions for the field in medium j. Their difference lies in the phase origin, taken in $u = u_j$ for the first and $u = u_j - e_j$ for the second.

C. Boundary Conditions and S Matrices

The unknown constant coefficients depend on two physical phenomena of different nature. On the one hand, crossing the interface, the total tangential field components are continuous, which implies that forward and backward waves are coupled. On the other hand, the propagation in a direction for which the medium remains constant creates only a dephasing or an attenuation without coupling between the two kinds of waves. The S-matrix formalism[15–17] is now well established for the study of modulated or planar stratified media. It is not affected by numerical instabilities linked to the number or the thickness of the layers. This is precisely because the boundary conditions are written by dividing the waves according to the propagation direction and not according to the propagation medium. For a given structure, the S matrix connects the incoming waves with the outgoing waves. Those qualifications have only a relative significance (see Figs. 3 and 4). In our problem the incoming waves consist only of the backward waves of the zeroth region, whereas the outgoing waves consist of the forward waves of the Qth region and the backward waves of the zeroth region. The sought $\mathbf{S}$ matrix is such that

$$\begin{pmatrix} A_{1\,pq}^{+0\ \mathrm{TE}} \\ A_{1\,pq}^{+0\ \mathrm{TM}} \\ A_{Q+1\,pq}^{-Q\ \mathrm{TE}} \\ A_{Q\ pq}^{-Q\ \mathrm{TM}} \end{pmatrix} = \mathbf{S} \begin{pmatrix} A_{1\,pq}^{-0\ \mathrm{TE}} \\ A_{1\,pq}^{-0\ \mathrm{TM}} \\ A_{Q+1\,pq}^{+Q\ \mathrm{TE}} \\ A_{Q\ pq}^{+Q\ \mathrm{TM}} \end{pmatrix}, \quad (58)$$

$$A_{Q\ pq}^{+Q\ \mathrm{TE}} = A_{Q\ pq}^{+Q\ \mathrm{TM}} = 0 \qquad \forall p \text{ and } \forall q, \quad (59)$$

$$A_{1\,pq}^{-0\ \mathrm{TE}} = \begin{cases} 0 & \text{if } p \text{ or } q \neq 0 \\ \cos\delta, & \text{if } p \text{ and } q = 0 \end{cases}, \quad (60)$$

$$A_{1\,pq}^{-0\ \mathrm{TM}} = \begin{cases} 0 & \text{if } p \text{ or } q \neq 0 \\ \sin\delta & \text{if } p \text{ and } q = 0 \end{cases}. \quad (61)$$

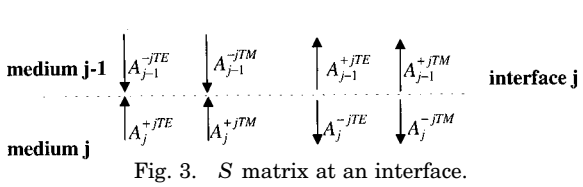

Fig. 3. S matrix at an interface.

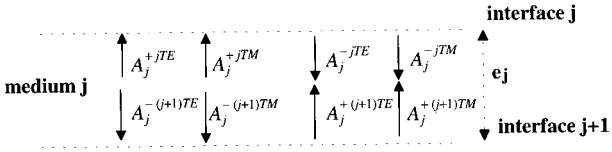

Fig. 4. S matrix of a layer.

1. Interface S Matrices

The tangential components of the field have to be continuous across the jth interface:

$$\psi_j^j(u_j) = \psi_{j+1}^j(u_j). \quad (62)$$

Following the S-matrix approach, we define an $S_{j-1,j}^j$ matrix by writing

$$\begin{pmatrix} \mathbf{A}_{j-1}^{+j\ \mathrm{TE}} \\ \mathbf{A}_{j-1}^{+j\ \mathrm{TM}} \\ \mathbf{A}_{j}^{-j\ \mathrm{TE}} \\ \mathbf{A}_{j}^{-j\ \mathrm{TM}} \end{pmatrix} = \mathbf{S}_{j-1,j}^{j} \begin{pmatrix} \mathbf{A}_{j-1}^{-j\ \mathrm{TE}} \\ \mathbf{A}_{j-1}^{-j\ \mathrm{TM}} \\ \mathbf{A}_{j}^{+j\ \mathrm{TE}} \\ \mathbf{A}_{j}^{+j\ \mathrm{TM}} \end{pmatrix}, \quad (63)$$

$$\mathbf{S}_{j-1,j}^{j} = (\boldsymbol{\psi}_{j-1}^{-j\ \mathrm{TE}}\ \boldsymbol{\psi}_{j-1}^{+j\ \mathrm{TM}}\ \boldsymbol{\psi}_{j}^{-j\ \mathrm{TE}}\ \boldsymbol{\psi}_{j}^{-j\ \mathrm{TM}})^{-1} \times (\boldsymbol{\psi}_{j-1}^{-j\ \mathrm{TE}}\ \boldsymbol{\psi}_{j-1}^{-j\ \mathrm{TM}}\ \boldsymbol{\psi}_{j}^{+j\ \mathrm{TE}}\ \boldsymbol{\psi}_{j}^{+j\ \mathrm{TM}}). \quad (64)$$

The $\mathbf{A}$ are column vectors of size L, with $L = (2M + 1) \times (2N + 1)$, the elements of which are the A_{pq}, and the $\boldsymbol{\psi}$ are the eigenvector matrices of size $4(L \times L)$. For example, we have

$$\boldsymbol{\psi}_j^{+j\ \mathrm{TE}} = (\boldsymbol{\psi}_{j\,pq}^{+j\ \mathrm{TE}}) = \begin{pmatrix} \mathbf{E}_{zj\,pq}^{+j} \\ \mathbf{H}_{xj\,pq}^{+j} \\ \mathbf{H}_{zj\,pq}^{+j} \\ \mathbf{E}_{xj\,pq}^{+j} \end{pmatrix}. \quad (65)$$

2. Layer S Matrices

In the jth medium, bounded by the jth and $(j + 1)$th interfaces, the scattered waves from one interface are the incident waves on the other one:

$$\begin{pmatrix} \mathbf{A}_{j}^{+j\ \mathrm{TE}} \\ \mathbf{A}_{j}^{+j\ \mathrm{TM}} \\ \mathbf{A}_{j}^{-(j+1)\ \mathrm{TE}} \\ \mathbf{A}_{j}^{-(j+1)\ \mathrm{TM}} \end{pmatrix} = \mathbf{S}_{j}^{j,j+1} \begin{pmatrix} \mathbf{A}_{j}^{-j\ \mathrm{TE}} \\ \mathbf{A}_{j}^{-j\ \mathrm{TM}} \\ \mathbf{A}_{j}^{+(j+1)\ \mathrm{TE}} \\ \mathbf{A}_{j}^{+(j+1)\ \mathrm{TM}} \end{pmatrix}, \quad (66)$$

with

$$\mathbf{S}_{j}^{i,j+1} = \begin{bmatrix} 0 & 0 & \varphi_j^{+} & 0 \\ 0 & 0 & 0 & \varphi_j^{+} \\ \varphi_j^{-} & 0 & 0 & 0 \\ 0 & \varphi_j^{-} & 0 & 0 \end{bmatrix}. \quad (67)$$

φ_j^{+} and φ_j^{-} are diagonal matrices, the elements of which are $\exp(-ikr_{j\,pq}^{+}e_j)$ and $\exp(ikr_{j\,pq}^{-}e_j)$, respectively.

The global S matrix is obtained through classical recursion formulas between the $\mathbf{S}_{j-1,j}^{j}$ and $\mathbf{S}_{j}^{j,j+1}$ matrices.

D. Diffraction Efficiencies

The application of Poynting's theorem, written in the translation coordinate system, enables us to calculate the power carried by the reflected and transmitted waves. Let us denote by N^u the contravariant u component of the complex Poynting vector:

$$N^u = \frac{1}{2}\,(E_z H_x^* - H_z^* E_x),$$

where H_x^* and H_z^* designate the complex conjugates of H_x and H_z, respectively.

In the jth medium, the time and surface average power carried by the (p, q) wave, $(p, q) \in U_j$, is given by

$$\begin{aligned} P_{j\,pq}^{\pm} &= \frac{1}{d_x}\frac{1}{d_z}\int_0^{d_x}\int_0^{d_z} N_{j\,pq}^{u\,\pm}\,\mathrm{d}x\mathrm{d}z \\ &= \frac{1}{2}\left(\sum_m \sum_n E_{zj\,mn\,pq}^{\pm\mathrm{TE}} H_{xj\,mn\,pq}^{*\pm\mathrm{TE}} - \sum_m \sum_n H_{zj\,mn\,pq}^{*\pm\mathrm{TE}} E_{xj\,mn\,pq}^{\pm\mathrm{TE}}\right) \\ &\quad + \frac{1}{2}\left(\sum_m \sum_n E_{zj\,mn\,pq}^{\pm\mathrm{TM}} H_{xj\,mn\,pq}^{*\pm\mathrm{TM}} - \sum_m \sum_n H_{zj\,mn\,pq}^{*\pm\mathrm{TM}} E_{xj\,mn\,pq}^{\pm\mathrm{TM}}\right). \end{aligned} \tag{68}$$

The efficiencies are defined as the ratio of these powers to that carried by the incident wave. In vacuum we obtain

$$e_{pq}^{r} = (|A_{0\,pq}^{+0\,\mathrm{TE}}|^2 + |A_{0\,pq}^{+0\,\mathrm{TM}}|^2)\,\frac{P_{0\,pq}^{+}}{P_{0\,pq}^{-}}, \tag{69}$$

and in the lowermost medium we obtain

$$e_{pq}^{t} = (|A_{Q\,pq}^{-Q\,\mathrm{TE}}|^2 + |A_{Q\,pq}^{+Q\,\mathrm{TM}}|^2)\,\frac{P_{Q\,pq}^{-}}{P_{0\,00}^{-}}. \tag{70}$$

4. NUMERICAL RESULTS

This section presents the results produced by the present code in some numerical experiments. We use a standard personal computer with a 200-MHz Pentium processor and 32-Mbyte memory. The program is implemented by using Matlab.

A. Testing the Computer Code and Comparison with Other Data

To show the advantage, in terms of computational speed, of the present formulation over my previous one, let us consider a perfectly conducting sinusoidal grating of the form

$$a(x, z) = \frac{h}{4}\left(\sin\frac{2\pi x}{d} + \sin\frac{2\pi z}{d}\right). \tag{71}$$

This grating is illuminated under normal incidence with a wavelength-to-period ratio $\lambda/d = 0.83$, and h/d is equal

Table 1. Comparison of the Computational Speed of the Codes Based on Two Formulations of the C Method[a]

	Present Formulation					Previous Formulation				
M, N	$e_{(-1,0)}^{r}$	$e_{(0,-1)}^{r}$	$e_{(0,0)}^{r}$	ϵ	Time (s)	$e_{(-1,0)}^{r}$	$e_{(0,-1)}^{r}$	$e_{(0,0)}^{r}$	ϵ	Time (s)
5	0.18318308	0.04441311	0.54480306	4.68×10^{-6}	31	0.18317513	0.04441197	0.54482602	2.39×10^{-7}	103
6	0.18318536	0.04441384	0.54480149	1.09×10^{-7}	81	0.18318483	0.04441374	0.544803	1.42×10^{-7}	274
7	0.18318539	0.04441385	0.54480151	2.17×10^{-9}	207	0.18318535	0.04441385	0.5448016	4.56×10^{-9}	673
8	0.18318538	0.04441385	0.54480152	1.3×10^{-11}	472	0.18318538	0.04441385	0.54480153	9×10^{-11}	1225

[a] The grating is the perfectly conducting sinusoidal crossed grating of Eq. (71) under normal incidence with a wavelength-to-period ratio $\lambda/d = 0.83$ and a height-to-period ratio $h/d = 1$.

Table 2. Comparison of the Numerical Results of the Present Study with the Results of Bruno and Reitich (Ref. 2) for the Perfectly Conducting Sinusoidal Crossed Grating of Eq. (71) under Normal Incidence with a Wavelength-to-Period Ratio $\lambda/d = 0.83$

	Ref. 2				Present Method ($M = N = 5$)			
h/d	$e_{(-1,0)}^{r}$	$e_{(0,-1)}^{r}$	$e_{(0,0)}^{r}$	ϵ	$e_{(-1,0)}^{r}$	$e_{(0,-1)}^{r}$	$e_{(0,0)}^{r}$	ϵ
0.1	0.01881	0.059691	0.842996	-6.6×10^{-16}	0.01881	0.05969	0.842996	2.22×10^{-16}
0.2	0.063551	0.192968	0.486961	-2.5×10^{-15}	0.063551	0.192968	0.486961	2.72×10^{-13}
0.3	0.110711	0.308565	0.161448	-6.0×10^{-13}	0.110711	0.308564	0.161448	4.18×10^{-11}
0.4	0.139786	0.342547	0.035335	-9.2×10^{-10}	0.139786	0.342547	0.035336	1.31×10^{-9}
0.5	0.134627	0.283651	0.163443	-1.6×10^{-7}	0.134627	0.283651	0.163443	1.57×10^{-8}
0.6	0.089612	0.168376	0.484016	-7.1×10^{-6}	0.089612	0.16838	0.484016	8.59×10^{-8}
0.7	0.036325	0.068458	0.790359	-7.1×10^{-5}	0.036319	0.068512	0.790338	1.92×10^{-7}
0.8	0.035293	0.033719	0.862052	7.8×10^{-5}	0.033869	0.035333	0.861597	4.59×10^{-8}
0.9	0.097266	0.04057	0.727476	3.1×10^{-3}	0.097905	0.039988	0.724214	1.15×10^{-7}
1	0.180165	0.048574	0.557739	1.5×10^{-2}	0.183183	0.044413	0.544803	4.68×10^{-6}

Table 3. Convergence Study of the Zero eflected Order for the Perfectly Conducting Sinusoidal Crossed Grating of Eq. (71), with Various Height-to-Period Ratios, under Normal Incidence with a Wavelength-to-Period Ratio $\lambda/d = 0.83$[a]

	Previous Formulation							
	$M = N = 5$		$M = N = 6$		$M = N = 7$		$M = N = 8$	
h/d	$e^r_{(0,0)}$	ϵ	$e^r_{(0,0)}$	ϵ	$e^r_{(0,0)}$	ϵ	$e^r_{(0,0)}$	ϵ
1	0.544826	-2.3×10^{-7}	0.544803	-1.4×10^{-7}	0.544802	-4.5×10^{-9}	0.544802	9×10^{-11}
1.1	0.41056	3.35×10^{-5}	0.410519	4.6×10^{-7}	0.410516	9×10^{-10}	0.410516	1.1×10^{-12}
1.2	0.32145	1.5×10^{-4}	0.321359	3.5×10^{-6}	0.321354	6.2×10^{-8}	0.321354	7.2×10^{-10}
1.3	0.24448	3.8×10^{-4}	0.244219	1×10^{-5}	0.244207	2.3×10^{-7}	0.244208	3.2×10^{-9}
1.4	0.15582	6.8×10^{-4}	0.155217	1.8×10^{-5}	0.15519	3.4×10^{-7}	0.155114	6.6×10^{-10}
1.5	0.77793	1.12×10^{-3}	0.77119	2.8×10^{-5}	0.77093	1.7×10^{-7}	0.077096	2.4×10^{-8}
1.6	0.05719	2.28×10^{-3}	0.0575	8.9×10^{-5}	0.05754	1.6×10^{-6}	0.05755	1.9×10^{-8}
1.7	0.09636	5.2×10^{-3}	0.09851	3.3×10^{-4}	0.09871	1.2×10^{-5}	0.098734	3.4×10^{-7}
1.8	0.16541	1×10^{-2}	0.169798	9×10^{-4}	0.170278	4.8×10^{-5}	0.17033	2×10^{-6}
1.9	0.248207	2×10^{-2}	0.255549	2.2×10^{-3}	0.256564	1.4×10^{-4}	0.256695	7.2×10^{-6}
2	0.350388	3.5×10^{-2}	0.362702	4.5×10^{-3}	0.364821	3.4×10^{-4}	0.365035	2×10^{-5}
	Present Formulation							
	$M = N = 5$		$M = N = 6$		$M = N = 7$		$M = N = 8$	
	$e^r_{(0,0)}$	ϵ	$e^r_{(0,0)}$	ϵ	$e^r_{(0,0)}$	ϵ	$e^r_{(0,0)}$	ϵ
	0.544803	4.68×10^{-6}	0.544801	1.09×10^{-7}	0.544802	2.17×10^{-9}	0.544802	1.3×10^{-11}
	0.410517	2.46×10^{-5}	0.410516	7.05×10^{-7}	0.410516	1.6×10^{-8}	0.410516	2.65×10^{-10}
	0.321369	7.7×10^{-5}	0.321354	2.7×10^{-6}	0.321354	7.2×10^{-8}	0.321355	1.5×10^{-9}
	0.244292	1.84×10^{-4}	0.24421	7.81×10^{-6}	0.244208	2.44×10^{-7}	0.244208	6.17×10^{-9}
	0.155435	4.05×10^{-4}	0.155201	2×10^{-5}	0.155195	7.34×10^{-7}	0.155195	2.04×10^{-8}
	0.077402	9.39×10^{-4}	0.077106	5.26×10^{-5}	0.077099	2.22×10^{-6}	0.077099	7.36×10^{-8}
	0.0575	2.19×10^{-3}	0.057538	1.38×10^{-4}	0.057553	6.66×10^{-6}	0.057554	2.43×10^{-7}
	0.097901	4.61×10^{-3}	0.098667	3.32×10^{-4}	0.098738	1.8×10^{-5}	0.098742	7.4×10^{-7}
	0.168347	8.68×10^{-3}	0.170154	7.17×10^{-4}	0.170337	4.38×10^{-5}	0.170344	2×10^{-6}
	0.252754	1.48×10^{-2}	0.256267	1.4×10^{-3}	0.256667	9.56×10^{-5}	0.256695	4.96×10^{-6}
	0.357264	2.3×10^{-2}	0.364129	2.48×10^{-3}	0.36501	1.87×10^{-4}	0.36508	1.1×10^{-5}

[a] It should be noted that an error has occurred in Ref. 9. In Table 2 on p. 787, the value of $e^r_{(0,0)}$ for $h/d = 2$ should read 0.36482 instead of 0.036482.

to 1. There are five reflected orders with $e^r_{(1,0)} = e^r_{(-1,0)}$ and $e^r_{(0,1)} = e^r_{(0,-1)}$ Table 1 lists the reflected efficiencies, the error in the energy balance, and the computational speed obtained with both formulations. The variable ϵ, which denotes the error in the energy balance, is defined as

$$\epsilon = 1 - \sum_{p,q \in U_0} e^r_{pq} - \sum_{p,q \in U_Q} e^t_{pq}.$$

Perfect energy balance does not necessarily indicate computational accuracy. However, concerning the C method, it has been previously observed,[9,14] by comparison with completely different methods, that the energy balance is a relevant criterion that gives a good indication of the accuracy of the results.

It is seen that the present formulation is some three times faster than the previous one.

For the same arrangement, we compare in Table 2 the reflected orders obtained with our new formulation and that of Bruno and Reitich[2] for various height-to-period ratios and truncation orders. It is seen that agreement is good for shallow gratings, but a growing discrepancy is observed when the groove depth is increased. To provide insight into the performance of the method, Table 3 presents the zero reflected order as a function of different groove depths for different truncation orders. The calculation is made with both our formulations. We see that accurate results are still observed for height-to-period ratios as high as 2 and that the present formulation is more precise than the previous one. Table 4 corresponds to a perfectly conducting pyramidal grating with depth-to-period ratio h/d = 0.5. It is illuminated under normal incidence with a wavelength-to-period ratio $\lambda/d = 0.4368$. In this case there are 21 reflected orders. Despite the slow convergence rate indicated by the ϵ parameter, accurate results are already obtained with M as small as 5. Table 5 shows the reflected and transmitted efficiencies of a dielectric pyramidal grating obtained with completely different formulations (Refs. 1, 4, 8, and 18). The parameters are $d_x = 1.5$, $d_z = 1$, $h = 0.25$, $\lambda = 1.533$, $\nu = 1.5$, $\theta = 30°$, $\phi = 45°$, and $\delta = 90°$. Figure 5 is for the gold grating from Fig. 7.17 of Ref. 11, which also corresponds

to Fig. 1 of Ref. 2. The refractive index of gold has been taken to be $\nu = 0.158 - i3.3986$. We observe a better agreement with the results of Ref. 11 than with those of Ref. 2.

B. Comparison with Experimental Data

Figures 6 and 7 show the numerical and experimental curves for reflectivity versus incident angle for a two-dimensional sinusoidal grating, the profile of which is described by Eq. (71). For this comparison experimental data were taken from a paper by Han *et al.*[19] Although it is not quite appropriate to compare theory and measurement for small reflectivity, we see a general agreement between measurements and predictions.

C. Application to Multilayer Diffraction

As a first example of multilayer crossed-grating diffraction, we consider a case where anomalies in the diffracted efficiencies occur. We consider a single layer bounded by vacuum. The profile consists of a sum of sinusoids. The parameters are layer thickness $e_2 = 337.49$ nm, $\upsilon_2 = 1.5$, $d_x = d_z = 600$ nm, $\lambda = 632.8$ nm, $\phi = 0$, and $h = 60$ nm. The condition on the guided-mode wave number of the corresponding unmodulated dielectric waveguide may be used to predict the range of the incident angle within which the resonances can be excited. For the above structure, one finds that the normalized propagation constant is equal to 1.3749 for the TE_0 mode and 1.3145 for the TM_0 mode. Assuming that coupling is due to the first evanescent order, the resonant angle should be equal to 18.67° for TE polarization and 15.06° for TM polarization. The reader interested in the details of the calculation of the resonant angle of incidence and in grating resonances is directed to Refs. 20–22. Figures 8 and 9 represent e^r_{00} efficiency versus θ for the TE and the TM polarization, respectively. It is seen that the resonance peaks occur at values slightly shifted from the preassumed ones because of the groove depth of the modulated layer.

To address the stability of the S-matrix approach, we consider a thick layer over the sinusoidal gold grating from Fig. 5. We deform the refractive index of the layer from its initial value to that of the gold substrate. Figure 10 represents the reflectivity of the above structure as a function of the period of the crossed grating for various values of the refractive index of the layer. When this reflectivity is that of the gold substrate, it can be seen that curve 3 of Fig. 10 coincides exactly with curve 3 of Fig. 5. Indeed, in that particular case, the structure is a simple crossed grating.

Finally, an example is given of diffraction by a grating with multiple overcoated layers. The coatings consist of alternating layers of zinc sulfite (ZnS) ($\nu = 2.37$) and cryolite (Na_3AlF_6) ($\nu = 1.35$) with a ZnS layer adjacent to the SiO_2 substrate ($\nu = 1.46$). It is assumed that all the coated layers have the same normalized thickness $\rho_j = 0.32$, with

$$\rho_j = e_j \nu_j / \lambda.$$

The grating profile is given by Eq. (71) with $h/d = 0.2$ and $\lambda/d = 0.8333$. The direction of the incident wave is chosen by imposing $\phi = \pi/4$ and the following relation:

Table 4. Convergence Study of the Efficiencies for a Perfectly Conducting Pyramidal Crossed Grating with $h = 0.5$, $d_x = d_z = 1$, $\theta = 0$, $\phi = 0$, $\delta = 90$, and $\lambda = 0.4368$

	$M = N = 5$	$M = N = 6$	$M = N = 7$	$M = N = 8$	$M = N = 9$	$M = N = 10$
$e^r_{(-1,-2)}$	0.027249	0.02727	0.027377	0.027393	0.027422	0.027428
$e^r_{(-0,-2)}$	0.037875	0.037428	0.037375	0.037287	0.037247	0.03721
$e^r_{(-2,-1)}$	0.028982	0.028708	0.028571	0.028477	0.02842	0.02838
$e^r_{(-1,-2)}$	0.005062	0.005115	0.005104	0.005115	0.005115	0.005118
$e^r_{(0,-1)}$	0.152897	0.154705	0.15546	0.155939	0.156184	0.156363
$e^r_{(-2-0)}$	0.036213	0.035908	0.035951	0.035922	0.035925	0.035916
$e^r_{(-1,,0)}$	0.139854	0.139041	0.138317	0.138054	0.137882	0.137798
$e^r_{(0,0)}$	0.019859	0.020346	0.020814	0.021003	0.021148	0.021229
ϵ	0.001291	0.001121	0.000768	0.000649	0.000549	0.000493

Table 5. Comparison among Different Methods for a Pyramidal Dielectric Grating with $d_x = 1.5$, $d_z = 1$, $h = 0.25$, $\lambda = 1.533$, $\nu = 1.5$, $\theta = 30°$, $\phi = 45°$, and $\delta = 90°$

					Present Method		
	Ref. 1	Ref. 8	Ref. 4	Ref. 18	$M = 3$	$M = 5$	$M = 7$
$e^r_{(-1,0)}$	0.00259	0.00254	0.00207	0.00249	0.00246	0.00246	0.00246
$e^r_{(0,0)}$	0.01948	0.01984	0.01928	0.01963	0.01962	0.01954	0.01951
$e^t_{(-1,-1)}$	0.00081	0.00092	0.00081	0.00086	0.00085	0.00086	0.00086
$e^t_{(0,-1)}$	0.00683	0.00704	0.00767	0.00677	0.00678	0.00679	0.00679
$e^t_{(-1,0)}$	0.00321	0.00303	0.0037	0.00294	0.00292	0.00294	0.00294
$e^t_{(0,0)}$	0.9643	0.96219	0.96316	0.96448	0.96493	0.96476	0.96472
$e^t_{(1,0)}$	0.00276	0.00299	0.00332	0.00282	0.00282	0.00281	0.0028
ϵ	0.00002	0.0013	−0.00001	0.00011	0.00019	0.00006	0.00009

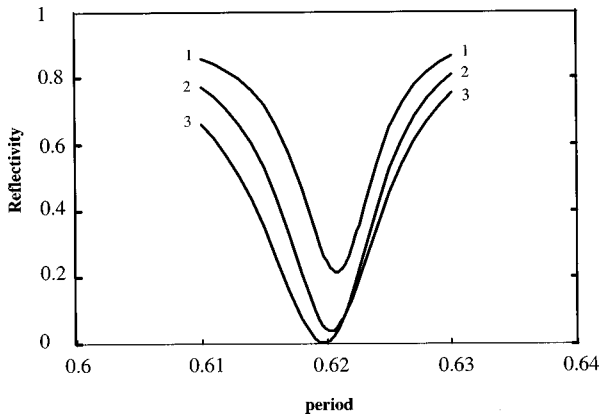

Fig. 5. Reflectivity versus period for a gold sinusoidal crossed grating with normally incident light of 0.65-μm wavelength. Curve 1, $h = 0.040\ \mu$m; curve 2, $h = 0.055\ \mu$m; curve 3, $h = 0.070\ \mu$m. $M = N = 2$.

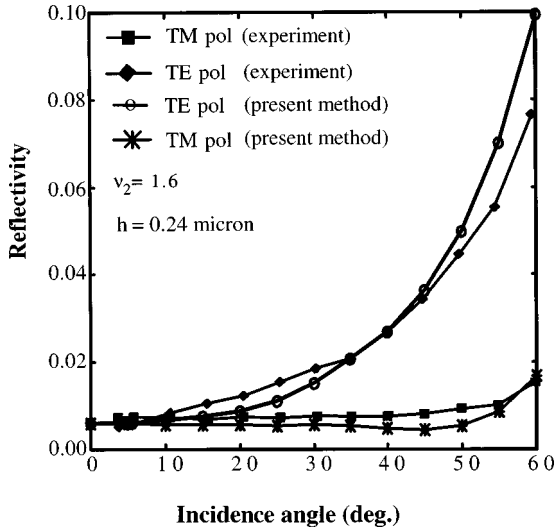

Fig. 6. Reflectivity versus incidence angle for a sinusoidal crossed grating with 3333 lines/mm along the x and z directions. $M = N = 4$. $\lambda = 632.8$ nm.

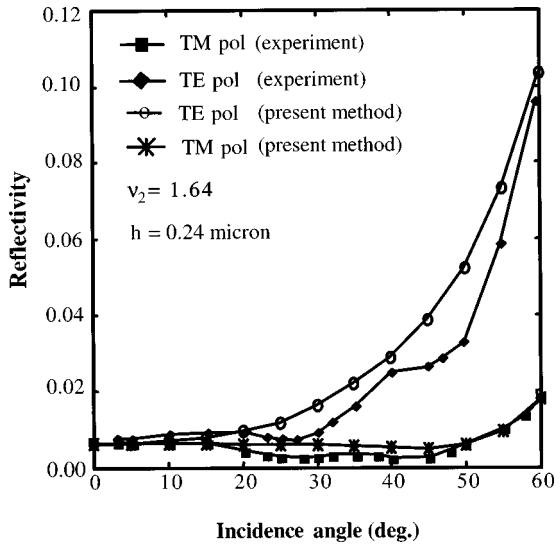

Fig. 7. Same as Fig. 6, but for a 3400-line/mm spacing.

$$\sin\theta = \frac{1}{\sqrt{2}}\frac{d}{\lambda}.$$

Hence the incident and the $(-1, -1)$ reflected order waves propagate along opposite directions. Table 6 lists the reflected efficiencies of a 22-layer coated grating. It is observed that only the TE polarization specular order exhibits a high efficiency. This numerical example

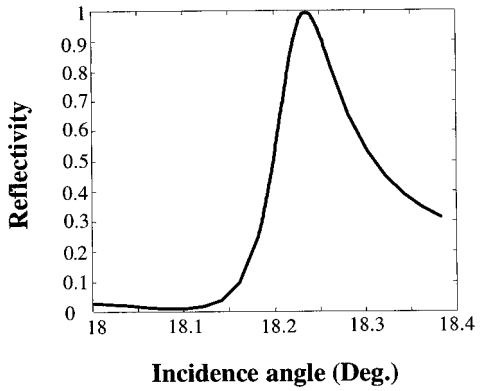

Fig. 8. Reflectivity versus incidence angle for a modulated layer bounded by vacuum. TE polarization case. $M = N = 3$.

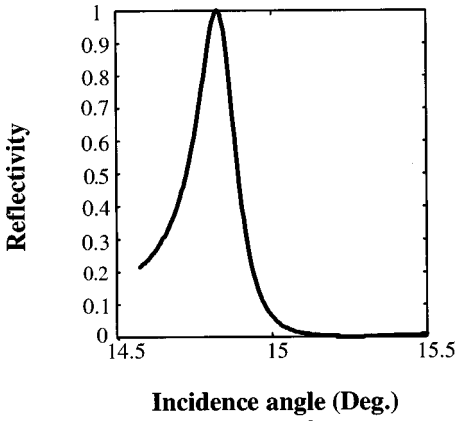

Fig. 9. Same as Fig. 8, but for the TM polarization case.

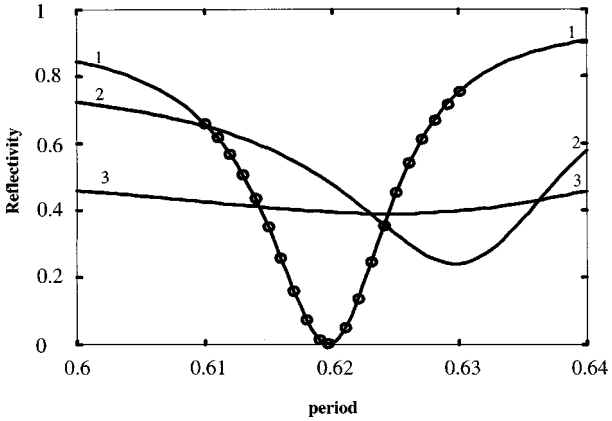

Fig. 10. Reflectivity versus period for a modulated layer above a gold substrate with normally incident light of 0.65-μm wavelength, with $e_1 = 1\ \mu$m and $h = 0.070\ \mu$m. Curve 1, $\nu_1 = 0.8 - i4$; curve 2, $\nu_1 = 1.5 - i3.3$; curve 3, $\nu_1 = 0.158 - i3.3986$. $M = N = 2$. The points marked by circles correspond to efficiencies calculated without the coating layer.

Table 6. Reflected Efficiencies of a 22-Layer Coated Grating

	$M = N = 3$	$M = N = 4$	$M = N = 5$
TE Polarization			
$e^r_{(-1,-1)}$	0.00371816	0.00379195	0.00379255
$e^r_{(0,-1)}$	0.0174459	0.01763833	0.01763991
$e^r_{(0,0)}$	0.79512396	0.79463043	0.79462637
ϵ	-7.4×10^{-7}	3.8×10^{-9}	-1.3×10^{-11}
TM Polarization			
$e^r_{(-1,-1)}$	0.03900172	0.03888695	0.0388858
$e^r_{(0,-1)}$	0.02094925	0.02104628	0.02104708
$e^r_{(0,0)}$	0.05357425	0.05366466	0.05366555
ϵ	2.6×10^{-5}	3.6×10^{-8}	3.6×10^{-10}

shows that the present code is capable of producing convergent results for gratings coated with many layers of total thickness reaching approximately 6 wavelengths.

5. CONCLUSION

An improved formulation of the Chandezon (C) method for crossed gratings was presented. It takes advantage of the polarization degeneracy of the eigenvalues of the initial problem. Very accurate results were obtained for large-depth-to-period-ratio gratings with a smooth profile. In addition, the S-matrix formalism was used to deal with multilayer crossed gratings. Hence we can investigate the properties of crossed gratings covered with a great number of modulated layers of any thickness. The main weakness of the C method lies in its difficulty to handle profiles with sharp edges. Thus the domain of validity is limited in terms of the geometry. However, for one-dimensional gratings and in particular cases, an oblique transformation[23] has overcome this difficulty. I believe that such transformations could also be helpful for two-dimensional gratings.

REFERENCES

1. P. Vincent, "A finite-difference method for dielectric and conducting crossed gratings," Opt. Commun. **26**, 293–296 (1978).
2. O. P Bruno and F. Reitich, "Numerical solution of diffraction problems: a method of variation of boundaries. III. Doubly periodic gratings," J. Opt. Soc. Am. A **10**, 2551–2562 (1993).
3. M. G. Moharam, "Coupled-wave analysis of two dimensional gratings," in *Holographic Optics: Design and Applications*, I. Cindrich, ed., Proc. SPIE **883**, 8–11 (1988).
4. R. Bräuer and O. Bryngdahl, "Electromagnetic diffraction analysis of two-dimensional gratings," Opt. Commun. **100**, 1–5 (1993).
5. E. Noponen and J. Turunen, "Eigenmode method for electromagnetic synthesis of diffractive elements with three-dimensional profiles," J. Opt. Soc. Am. A **11**, 2494–2502 (1994).
6. S. Peng and G. M. Morris, "Efficient implementation of rigorous coupled-wave analysis for surface-relief gratings," J. Opt. Soc. Am. A **12**, 1087–1096 (1995).
7. L. Li, "New modal method by Fourier expansion for crossed surface-relief gratings," J. Opt. Soc. Am. A **14**, 2758–2767 (1997).
8. G. H. Derrick, R. C. McPhedran, D. Maystre, and M. Nevière, "Crossed gratings: a theory and its applications," Appl. Phys. **18**, 39–52 (1979).
9. G. Granet, "Diffraction par des surfaces bipériodiques: résolution en coordonnées non orthogonales," Pure Appl. Opt. **4**, 777–793 (1995).
10. J. B. Harris, T. W. Preist, J. R. Sambles, R. N. Thorpe, and R. A. Watts, "Optical response of bigratings," J. Opt. Soc. Am. A **13**, 2041–2049 (1996).
11. R. C. McPhedran, G. H. Derrick, and L. C. Botten, "Theory of crossed gratings," in *Electromagnetic Theory of Gratings*, R. Petit, ed. (Springer-Verlag, Berlin, 1980), Chap. 7.
12. R. F. Harrington, *Time-Harmonic Electromagnetic Fields* (McGraw-Hill, New York, 1961).
13. E. J. Post, *Formal Structure of Electromagnetics* (North-Holland, Amsterdam, 1962).
14. J. Chandezon, M. T. Dupuis, G. Cornet, and D. Maystre, "Multicoated gratings: a differential formalism applicable in the entire optical region," J. Opt. Soc. Am. A **72**, 839–847 (1982).
15. N. P. K. Cotter, T. W. Preist, and J. R. Sambles, "Scattering-matrix approach to multilayer diffraction," J. Opt. Soc. Am. A **12**, 1097–1103 (1995).
16. G. Granet, J. P. Plumey, and J. Chandezon, "Scattering by a periodically corrugated dielectric layer with non-identical faces," Pure Appl. Opt. **4**, 1–5 (1995).
17. L. Li, "Formulation and comparison of two recursive matrix algorithms for modeling layered diffraction gratings," J. Opt. Soc. Am. A **13**, 1024–1034 (1996).
18. J. J. Greffet, C. Baylard, and P. Versaevel, "Diffraction of electromagnetic waves by crossed gratings: a series solution," Opt. Lett. **17**, 1740–1742 (1992).
19. S. T. Han, Y. Tsao, R. M. Walser, and M. F. Becker, "Electromagnetic scattering of two-dimensional surface-relief dielectric gratings," Appl. Opt. **31**, 2343–2352 (1992).
20. E. Popov, L. Mashev, and D. Maystre, "Theoretical study of the anomalies of coated dielectric gratings," Opt. Acta **33**, 607–619 (1986).
21. S. S. Wang and R. Magnusson, "Theory and applications of guided-mode resonance filters," Appl. Opt. **32**, 2606–2613 (1993).
22. S. Peng and G. M. Morris, "Resonant scattering from two-dimensional gratings," J. Opt. Soc. Am. A **13**, 993–1005 (1996).
23. J. P. Plumey, B. Guizal, and J. Chandezon, "The coordinate transformation method as applied to asymmetric gratings with vertical facets," J. Opt. Soc. Am. A **14**, 610–617 (1997).